

Winning Solution of Real Robot Challenge III

Qiang Wang, Robert McCarthy, David Cordova Bulens, and Stephen J. Redmond

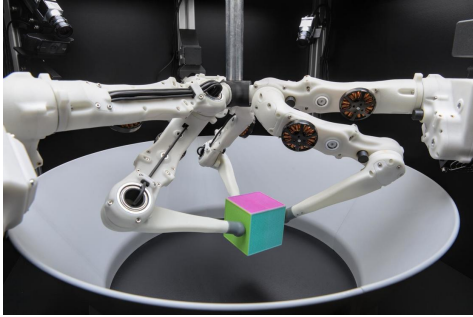
October 2022

Abstract

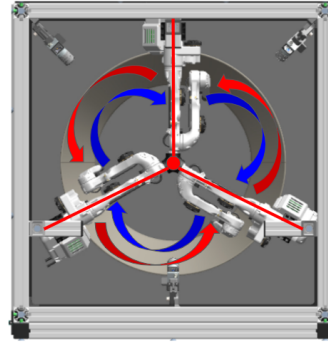
This report introduces our winning solution of the real-robot phase of the Real Robot Challenge (RRC) 2022. The goal of this year’s challenge is to solve dexterous manipulation tasks with offline reinforcement learning (RL) or imitation learning. To this end, participants are provided with datasets containing dozens of hours of robotic data. For each task an *expert*¹ dataset and a *mixed* dataset are provided. In our experiments, when learning from the *expert* datasets, we find standard Behavioral Cloning (BC) outperforms state-of-the-art offline RL algorithms. When learning from the *mixed* datasets, BC performs poorly, as expected, while surprisingly offline RL performs suboptimally, failing to match the average performance of the baseline model used for collecting the datasets. To remedy this, motivated by the strong performance of BC on the *expert* datasets we elect to use a semi-supervised classification technique to filter the subset of *expert* data out from the *mixed* datasets, and subsequently perform BC on this extracted subset of data. To further improve results, in all settings we use a simple data augmentation method that exploits the geometric symmetry of the RRC physical robotic environment. Our submitted BC policies each surpass the mean return² of their respective raw datasets, and the policies trained on the filtered *mixed* datasets come close to matching the performances of those trained on the *expert* datasets.

1 Real Robot Challenge 2022

Data-driven learning methods are promising for dexterous robotic manipulation tasks - they can learn complex, skillful manipulation strategies from scratch, and indeed have begun to outperform more traditional control methods in some settings (CITE). However, learning manipulation policies from real robots usually involves costly and time-consuming data collection. However, these issues can potentially be mitigated by making use of available pre-collected data. The RRC 2022 seeks to encourage the development of offline algorithms that can make efficient use of such real-world data, and thus improve the performance of our learning methods when applied in practical real-world scenarios.



(a) The real TriFinger robot used in the RRC 2021.



(b) The top view of the robot arena.

Figure 1: The TriFinger robot[21]. Three identical robotic fingers are equally spaced around the circular arena. The colored cube is the target object that must be moved.

In the RRC 2022, participant are provided with dozens of hours of TriFinger[21] robotic data. Datasets are provided for two robotic tasks, *push* and *lift*. In the *push* task, the cube must be moved to target positions on the arena floor. In the more challenging *lift* task, the cube must be lifted and maintained at a target position and orientation. For each task, two separate datasets are provided; one collected by an *expert* policy (the *expert* dataset), the other collected by a number of policies with various skill levels (*mixed* dataset). Thus, there are four separate datasets. Participants must submit a different policy for each respective dataset. Only learning-based approaches are permitted, and datasets cannot be combined in the training process. Access is also provided to a cluster of real TriFinger robots (see Figure1(a)) to allow participants to evaluate their trained policies; however, data from the evaluation, either performed in simulation or on the real robot, is not allowed to be used to further refine a policy. For more details, please see the official website of RRC³. We now describe our approach to the challenge.

¹For convenience, we name the datasets collected by *expert* policies as the *expert* dataset and the data contained within it as *expert* data. For the dataset collected by *mixed* policies, we name it the *mixed* dataset and the data contained within it *mixed* data.

²The cumulative reward acquired in each episode.

³<https://real-robot-challenge.com/protocol>

Table 1: Real-robot evaluated score comparison of algorithms trained from both *expert* and *mixed* dataset of the *lift* task, where the Baseline refers to the mean episodic return in the dataset.

	BC	BCQ	PLAS	IQL	Ours	Baseline
<i>Lift</i> exp	928.91	646.18	911.91	789.12	1129.70	1064.00
<i>Lift</i> mix	489.25	432.75	711.28	550.23	998.82	851.00

2 Methodology

2.1 Our approach

In our experiments we found that standard BC outperforms a number of state-of-the-art offline reinforcement learning algorithms⁴ on the *lift expert* dataset. Specifically, the offline reinforcement learning algorithms we tested included Batch-Constrained Q-learning (BCQ)[17], Policy in Latent Action Space (PLAS)[18], and Implicit Q-Learning (IQL)[19]. The evaluated results of these algorithms on the *lift* task are compared in Table 1.

Now, when experimenting on the *mixed* dataset, we find both standard BC and offline RL to perform relatively poorly, failing to reach the mean returns of the dataset in all cases. BC’s poor performance is to be expected – the *mixed* dataset presents two challenges for BC:

1. It contains a large number of less successful episodes (see Figure 2); imitating the behaviour in these episodes will hurt performance.
2. It contains data collected by multiple policies; i.e., the data when sorted by summed reward over the episode is multi-modal (see Figure 2). Unless accounted for explicitly, a naive BC approach may perform poorly on a multi-modal dataset[16], even if the data is of high quality, as it is trying to find a single policy that can replicate the behaviour of two or more very different policies.

Offline RL should in theory be capable of learning *expert* behaviour from such a *mixed* dataset, and indeed the tested algorithms outperform BC, however, performance is still suboptimal.

Data filtering: Motivated by the strong performance of BC on the *expert* dataset, we attempt to improve results on the *mixed* dataset by splitting the *mixed* dataset into subsets, where each subset contains the data from a single policy, and we subsequently apply BC to the subset of data came from the best-performing policy. Note, we find the approach of naively splitting the dataset into two subsets based on reward returns (for example, from where the red arrow points in Figure 2(b)) and applying BC to the subset with higher rewards leads to poor performance. Here, the subset sorted by summed reward is still multimodal, containing a number of higher reward episodes collected by the weaker policies. Many of these episodes collected by weaker policies can be further filtered out by increasing the reward return threshold (like Eq. 1), ensuring that almost all of the filtered data is collected by the higher performing policy. However, we find this new subset is then too small to train a BC model with good performance. Therefore, we propose a semi-supervised data filtering approach which can effectively extract the data collected by the best performing policy (*expert* policy) from the *mixed* dataset.

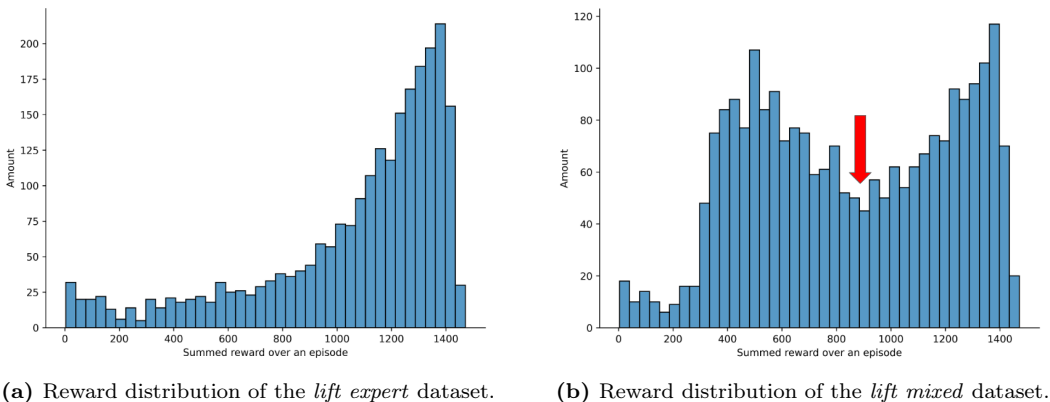


Figure 2: The histogram of the accumulated reward over an episode, calculating by summing all rewards of each episode together. The *expert* dataset consists mostly of successful episodes, in which the cube was moved to the target. The *mixed* dataset appears to consist two distinct peaks, therefore, we assume that the *mixed* dataset is collected jointly by at least two policies, at least one of which is an *expert*.

⁴We primarily make use of algorithms implemented in the d3rlpy library[15]

Method summary: In summary, for our final submissions, we use BC-based approaches in all cases. On the *mixed* datasets we use our data filtering approach to extract the *expert* data and use it to train the BC policy. As a supervised learning algorithm, the BC is affected by the compound error led by the covariate shift[16]. The root cause is that the trained BC model encounters many unseen data during deployment. One solution is to increase the training dataset size; hence, to further enhance performances we also introduce a data augmentation method that exploits the symmetry of the robot environment using simple rotational transforms, which can increase the amount of the training data by three times. We describe these methods in more detail in the next section.

2.2 Expert data filter

A data filter (i.e., a binary classifier that assigns a label to an epoch) is trained and applied to the *mixed* dataset to extract the data collected by the/an *expert* policy. Figure 3 shows the filter training process, which includes: 1) First filtering the raw dataset such that only a small subset of the highest return episodes are retained (see section 2.2.2) to form a *superb* dataset, which is small, but, we expect, mostly consists of data collected by the *expert* policy; 2) Use the *superb* dataset to pre-train the filter classifier; 3) Use the trained (or pre-trained) filter classifier to relabel the entire dataset, and then use the relabelled dataset to retrain the filter classifier again; 4) Repeat step 3 until the filtered dataset’s membership does not change or vary, within some reasonable tolerance.

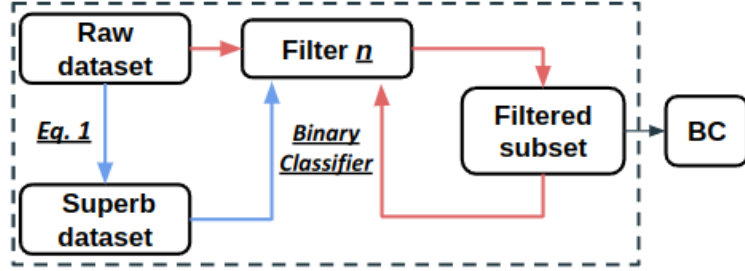


Figure 3: Filter training flow chart, where the blue arrows indicate the pre-training process and the red arrows indicate one iteration of the process of training the filter.

2.2.1 Structure of the filter

Figure 4 shows the filter’s structure, which is a classifier that outputs the binary prediction indicating whether the input data was collected by using an *expert* policy, or not. The significant dimensional gap between the observation and the action may result in data bias; hence the dimension of the observation vector is reduced before concatenating with the action vector. The classifier operates on vectors from a single time-step; then, a post-processing step is performed by aggregating the classifier-applied label across all time-steps in one episode to get a final label. This is done by summing the binary labels across all time-steps and then applying a threshold, where the threshold is selected by observing the performance of BC trained from the filtered subset.

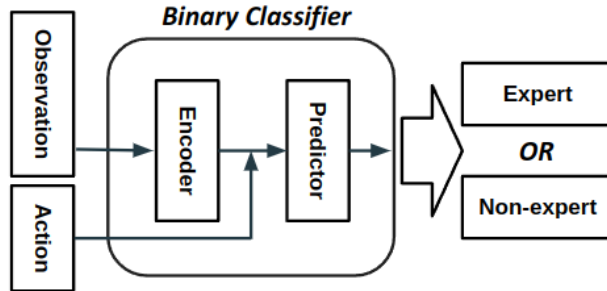


Figure 4: The structure of the filter. The encoder and predictor are fully-connected neural networks; the architecture is shown in Appendix A.1.

2.2.2 Generate the training data

The *expert* and *non-expert* policy have significantly different summed reward when the episode has a high difficulty. For this reason, the *superb* dataset was formed using the criterion presented in Eq. 1:

$$ExpertEpisode = \begin{cases} True, & \text{if } (\mathbb{E}(R[t_{start}]) \leq th_{low}) \text{ AND } (\mathbb{E}(R[t_{end}]) \geq th_{high}) \\ False, & \text{otherwise} \end{cases} \quad (1)$$

where R is the episodic reward⁵, a set of values, with each value for the reward of each time-step. And the expectation operator \mathbb{E} is implemented by taking the sample mean. t_{start} is the set of time indices addressing reward value for the first five time-steps in the episode. t_{end} is the set of time indices addressing reward value for the last 150 time-steps in the episode. th_{low} value is 0.33 for both tasks, and th_{high} value for the *lift* task is 0.98, and for the *push* task is 0.96. The first constraint (to the left of the logical AND in Eq. 1) makes only the relatively challenging episodes be chosen by taking those with lower average rewards over the initial five time-steps, which removes episodes where the cube started at or near the target. The second constraint (to the right of the logical AND in Eq. 1) is set to choose episodes with excellent behavioural quality by taking those having high average rewards over the final 150 time-steps. The second constraint is based on the assumption that if rewards are high throughout the end of episode, then the agents has performed the task well. Hence, by combining both constraints, we only keep difficult episodes where the agent manages to successfully completes them; it is highly possible to make the vast majority of the filtered episodes collected by the *expert*. The setting of the above constants(t_{start} , t_{end} , th_{low} , th_{high}) performs the best over our attempts. In the beginning, we roughly set reasonable values for the above constants, enabling the classifier’s training on the superb dataset to converge. Afterwards, we fine-tune these values based on observing the loss during the classifier’s training(smaller converged loss and smoother loss curve means the threshold is better) and the evaluated score of BC trained from the final filtered subset.

We name the data from either the *superb* and filtered subset as labelled *EXPERT*; that is, coming from an *expert* policy. We propose two ways to generate *NON-EXPERT*-labelled training data, which we consider to not come from an *expert* policy, shown in Figure 5. 1) Combine the observations of *EXPERT* samples with the actions in the part of data that is not filtered. 2) Combine the observations of *EXPERT* samples with randomly-generated action data. Only the actions with a relatively larger difference from the *EXPERT* actions can be deemed as negative; this reduces the overall similarity between *NON-EXPERT* and *EXPERT* training samples and thus encourages the learning of the filter.

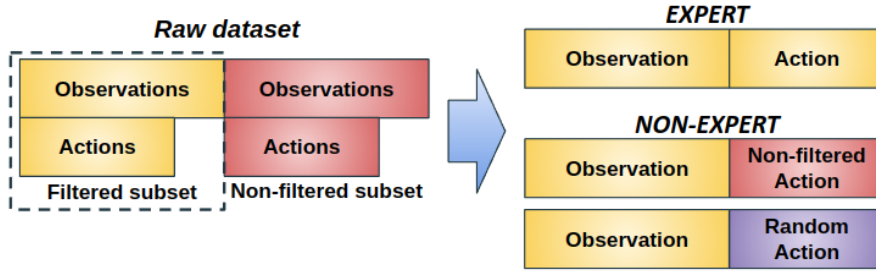


Figure 5: The illustration of generating the *EXPERT* and *NON-EXPERT* samples for training the filter. The filtered subset involves the data filtered by both Eq. 1 and the trained classifier filter. The Non-filtered subset is the raw dataset that excludes the Filtered subset.

2.2.3 Filter process

The filter is a binary classifier, which takes the SOFTMAX function as the last-layer activation function. One of SOFTMAX’s outputs estimates the probability that the episode is *expert*-collected. In the filtering phase, we feed the raw dataset into the filter network to obtain the estimated probabilities of being *expert* of each time-step and sum them in each episode. This summed probability value is called the **confidence** that one episode is *expert*-collected. When the **confidence** of one episode is greater than a specific threshold th_{conf} , it is deemed a *EXPERT* episode.

The selection of the th_{conf} value may lead to results with a significant difference, which is determined by both reasonable hypotheses and observing the evaluated score of BC trained from the final filtered subset. Our experiment found that the output **confidence** is large over most episodes at the beginning of the iterations⁶, with most of the episodes in the *lift mixed* dataset having **confidence** in the range 1100-1500(max possible **confidence** is 1500)⁷, and that of the *push mixed* dataset is 650-750 (max possible **confidence** is 750)⁸. This is led by the high similarity between the *EXPERT* and *NON-EXPERT* samples since they share the same observations in the filtered subset, as seen in Figure 5. Hence, we set a relatively large th_{conf} at the beginning of the iterations, which of the *lift mixed* dataset is 1420 and the *push mixed* dataset is 730. At the end of the iterations, we found that the **confidence** of a big part of episodes becomes smaller; we reasonably guess this is because the filter classifier becomes more robust, hence clarifying the *NON-EXPERT* more clearly. Therefore, to filter the final subset for training the BC, we set the th_{conf} to a relatively smaller value making more episodes can be chosen, which of the *lift mixed* dataset is 1390 and the *push mixed* dataset is 500. Same as above, this settings of th_{conf} performs the best over our attempts. In the beginning, we roughly set reasonable values through assumption and then we fine-tune these values based on observing the evaluated score of BC trained from the final filtered subset.

⁵The method for calculating the reward of each time-step in the dataset was designed by the organizer and can be found in the RRC documentation: <https://webdav.tuebingen.mpg.de/real-robot-challenge/2022/docs/tasks.html#rewards-and-success>

⁶The classifier filter is repeatedly trained by the latest filtered subset mentioned above at the beginning of 2.1. We name each repeat process iteration.

⁷The episodic length of *lift* task is 1500

⁸The episodic length of *push* task is 750

2.3 Data augmentation through rotational transformation

The top view of the robotic arena is shown in Figure 1(b). Three fingers of the robot are placed evenly around the center of the rounded working platform with an angle difference between the nearby two fingers of 120° . Since the structure of each finger is identical, theoretically, the correctness of the data, including the states of the object and fingers, remains unchanged after rotating clockwise (blue arrows in Figure 1(b)) or counterclockwise (red arrows in Figure 1(b)) around the central point of the arena by 120° . We divided observations into robot and object states⁹ and conducted the following mathematical calculations for augmentation:

Robot state The state data of the robot is augmented by cycling the state data around the fingers:

$$\mathbf{FingerState}(\theta) = \mathbf{FingerState}(\theta + k \cdot 120^\circ) \quad (2)$$

where $\theta \in (0^\circ, 120^\circ, 240^\circ)$ and $k \in (0, 1, 2)$. For example, the state data of the robot will be rotated 120° clockwise when k is 1.

Object state The x-y Cartesian coordinates of the object state is rotationally transformed by:

$$\begin{bmatrix} \mathbf{Obj}_{x'} \\ \mathbf{Obj}_{y'} \end{bmatrix} = \begin{bmatrix} \cos(k \cdot 120^\circ) & -\sin(k \cdot 120^\circ) \\ \sin(k \cdot 120^\circ) & \cos(k \cdot 120^\circ) \end{bmatrix} \cdot \begin{bmatrix} \mathbf{Obj}_x \\ \mathbf{Obj}_y \end{bmatrix} \quad (3)$$

where \mathbf{Obj}_x and \mathbf{Obj}_y are the \mathbf{xy} coordinates values of the object and $k \in (0, 1, 2)$. The z coordinate of the object stays the same because the rotation transformation is conducted on the horizontal plane (the arena floor).

The data after rotational transformation is concatenated with the original data to form a large augmented dataset.

2.4 Train & tune

The precision of the above augmentation approach only stands in the theoretical robotic system, which is not possible in the real world since the physical parameters between each finger are slightly different. Hence, we first trained a BC model with the large augmented dataset, which can alleviate the issue led by the compound error and acquire a more general policy. Then the trained model is tuned on the actual data (before augmentation) at a lower learning rate, making the final deployed BC model a better fit for the real-robot data distribution.

The neural network’s architecture of both BC and filter, and training parameters are given in the Appendix A.1. Because the RRC dataset is large, our approach for processing the *mixed* datasets requires a machine with 16 GB RAM, whereas for the *expert* datasets we require 32 GB. Our experiments of *mixed* dataset ran on a PC with an Intel I7-10875H CPU (2.30 GHz \times 16, 16 GB RAM) and an NVIDIA 2060 GPU (6 GB RAM). Moreover, our experiments of the *expert* datasets ran on Sonic high-performance cluster at University College Dublin, where the machines are configured with 2 Intel Xeon Gold 6152 CPUs (2.1 GHz \times 22, 64 GB RAM).

Table 2: Real-robot evaluated scores of our approach and standard BC, where the *Train&Tune* is our full final approach

	<i>Push expert</i>	<i>Push mixed</i>	<i>Lift expert</i>	<i>Lift mixed</i>
Standard BC	628.12	497.26	928.65	469.25
<i>Train&Tune</i>	662.30	636.49	1129.70	998.82
Baseline	660.00	429.00	1064.00	851.00

3 Results and Discussion

On *expert* datasets, our *train & tune* method effectively improves the BC models’ performance (see Table 2), demonstrating the effectiveness of our augmentation approach. Our approach can be extended to tasks with specific geometry properties, such as symmetry, and it effectively increases the data utilization efficiency. However, due to the theory-to-real gap, the data inferred from mathematics may shift from the actual robotic data distribution, resulting in a mismatch between the trained policy by the augmented dataset and the robot. Hence the policy should be tuned on non-augmented data before deployment to make the trained model fit the actual robotic environment.

The BC models trained jointly by our filter and *train & tune* approach on the *mixed* dataset acquire the mean return close to that in the *expert* dataset in the evaluation stage. They outperform the baselines, which demonstrates the effectiveness of our proposed filter method.

⁹More details about the observation space see <https://webdav.tuebingen.mpg.de/real-robot-challenge/2022/docs/tasks.html>

4 Conclusion

Our approach dramatically improves the performance of BC on both *expert* and *mixed* datasets, which exceeds the baselines in all tasks and has reasonable generalization capability. In our future work, we will integrate the filter’s iterative training process with the controller policy’s training process to avoid the complex iterative process of filtering.

References

- [1] Mnih, V., Kavukcuoglu, K., Silver, D., Graves, A., Antonoglou, I., Wierstra, D. and Riedmiller, M., 2013. Playing Atari with deep reinforcement learning. arXiv preprint arXiv:1312.5602.
- [2] Lillicrap, T.P., Hunt, J.J., Pritzel, A., Heess, N., Erez, T., Tassa, Y., Silver, D. and Wierstra, D., 2015. Continuous control with deep reinforcement learning. arXiv preprint arXiv:1509.02971.
- [3] Schulman, J., Wolski, F., Dhariwal, P., Radford, A. and Klimov, O., 2017. Proximal policy optimization algorithms. arXiv preprint arXiv:1707.06347.
- [4] Haarnoja, T., Zhou, A., Abbeel, P. and Levine, S., 2018, July. Soft actor-critic: Off-policy maximum entropy deep reinforcement learning with a stochastic actor. In International conference on machine learning (pp. 1861-1870). PMLR.
- [5] Ha, D. and Schmidhuber, J., 2018. World models. arXiv preprint arXiv:1803.10122.
- [6] Hafner, D., Lillicrap, T., Fischer, I., Villegas, R., Ha, D., Lee, H. and Davidson, J., 2019, May. Learning latent dynamics for planning from pixels. In International Conference on Machine Learning (pp. 2555-2565). PMLR.
- [7] Levine, S., Kumar, A., Tucker, G. and Fu, J., 2020. Offline reinforcement learning: Tutorial, review, and perspectives on open problems. arXiv preprint arXiv:2005.01643.
- [8] Hussein, A., Gaber, M.M., Elyan, E. and Jayne, C., 2017. Imitation learning: A survey of learning methods. ACM Computing Surveys (CSUR), 50(2), pp.1-35.
- [9] Ho, J. and Ermon, S., 2016. Generative adversarial imitation learning. Advances in Neural Information Processing Systems, 29.
- [10] Ng, A.Y. and Russell, S., 2000, June. Algorithms for inverse reinforcement learning. In ICML (Vol. 1, p. 2).
- [11] Wang, Q., Sanchez, F.R., McCarthy, R., Bulens, D.C., McGuinness, K., O’Connor, N., Wüthrich, M., Widmaier, F., Bauer, S. and Redmond, S.J., 2022. Dexterous Robotic Manipulation using Deep Reinforcement Learning and Knowledge Transfer for Complex Sparse Reward-based Tasks. arXiv preprint arXiv:2205.09683.
- [12] McCarthy, R., Sanchez, F.R., Wang, Q., Bulens, D.C., McGuinness, K., O’Connor, N. and Redmond, S.J., 2021. Solving the real robot challenge using deep reinforcement learning. arXiv preprint arXiv:2109.15233.
- [13] Ross, S. and Bagnell, D., 2010, March. Efficient reductions for imitation learning. In Proceedings of the thirteenth international conference on artificial intelligence and statistics (pp. 661-668). JMLR Workshop and Conference Proceedings.
- [14] Ross, S., Gordon, G. and Bagnell, D., 2011, June. A reduction of imitation learning and structured prediction to no-regret online learning. In Proceedings of the fourteenth international conference on artificial intelligence and statistics (pp. 627-635). JMLR Workshop and Conference Proceedings.
- [15] Seno, T. and Imai, M., 2021. d3rlpy: An Offline Deep Reinforcement Learning Library. arXiv preprint arXiv:2111.03788.
- [16] Lecture2: Supervised Learning and Behaviour of Deep Reinforcement Learning tutorial. Available at: <http://rail.eecs.berkeley.edu/deeprlcourse-fa21/static/slides/lec-2.pdf> (Accessed: 9 Oct 2022).
- [17] Fujimoto, S., Meger, D. and Precup, D., 2019, May. Off-policy deep reinforcement learning without exploration. In International Conference on Machine Learning (pp. 2052-2062). PMLR.
- [18] Zhou, W., Bajracharya, S. and Held, D., 2020. Plas: Latent action space for offline reinforcement learning. arXiv preprint arXiv:2011.07213.
- [19] Kostrikov, I., Nair, A. and Levine, S., 2021. Offline reinforcement learning with implicit Q-learning. arXiv preprint arXiv:2110.06169.
- [20] Kingma, D.P. and Ba, J., 2014. Adam: A method for stochastic optimization. arXiv preprint arXiv:1412.6980.
- [21] Wüthrich, M., Widmaier, F., Grimminger, F., Akpo, J., Joshi, S., Agrawal, V., Hammoud, B., Khadiv, M., Bogdanovic, M., Berenz, V. and Viereck, J., 2020. Trifinger: An open-source robot for learning dexterity. arXiv preprint arXiv:2008.03596.

A Neural network

We implemented the BC by referencing d3rlpy[15]. Our implementations of both BC and filter will be open-sourced on GitHub: <https://github.com/wq13552463699/Real-Robot-Challenge-2022.git> after RRC2022.

A.1 Architecture

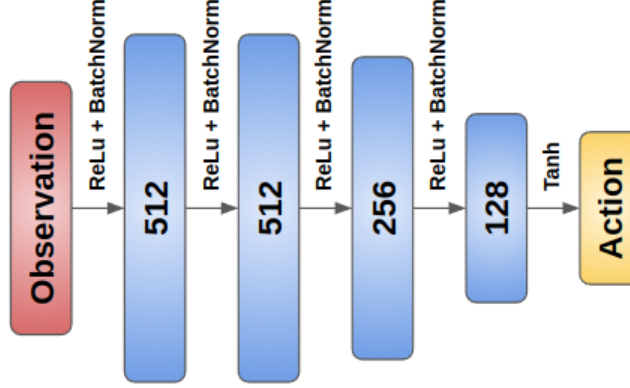
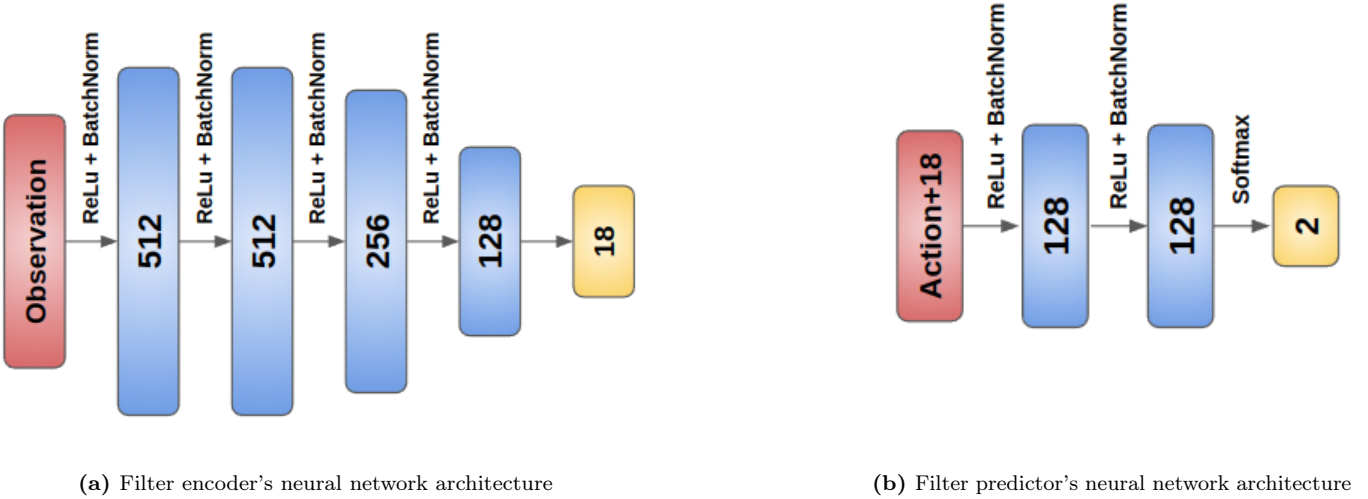


Figure 6: Behaviour Cloning model’s neural network architecture



(a) Filter encoder’s neural network architecture

(b) Filter predictor’s neural network architecture

Figure 7: The neural network architectures of two separated components of the filter

A.2 Hyper-parameter

A.2.1 BC

Train The training of BC in our approach includes *train* & *tune*. In the *Train* stage, we used Adam[20] for learning the neural network parameters with the learning of 10^{-3} , where the weight decay was not included. The *Train* process lasted 50 epochs with a batch size of 1024. The hyperparameter of the *Tune* stage is the same as *Train*, except the learning rate is 8×10^{-4} .

A.2.2 Filter

The filter training for the *push mixed* dataset lasts 3 iteration, while the *lift mixed* dataset is 4. For each iteration, we used Adam[20] for learning the neural network parameters with the learning of 10^{-3} , where the weight decay was not included. The training process lasted 50 epochs with a batch size of 1024.